HHS Public Access

Author manuscript

Cancer Res. Author manuscript; available in PMC 2020 August 01.

Published in final edited form as:

Cancer Res. 2019 August 01; 79(15): 3940–3951. doi:10.1158/0008-5472.CAN-19-0761.

Inhibition of ATM increases interferon signaling and sensitizes pancreatic cancer to immune checkpoint blockade therapy

Qiang Zhang[1,*], **Michael D. Green**[1,2,*], **Xueting Lang**[3], **Jenny Lazarus**[3], **Joshua D. Parsels**[1], **Shuang Wei**[3], **Leslie A. Parsels**[1], **Jiaqi Shi**[4], **Nithya Ramnath**[5], **Daniel R. Wahl**[1], **Marina Pasca di Magliano**[3], **Timothy L. Frankel**[3], **Ilona Kryczek**[3], **Yu Lei**[6,7], **Theodore S. Lawrence**[1], **Weiping Zou**[2,3,4,7,†], **Meredith A. Morgan**[1,†]

[1]Department of Radiation Oncology, University of Michigan Rogel Cancer Center, University of Michigan School of Medicine, Ann Arbor, Michigan, USA.

[2]Center of Excellence for Cancer Immunology and Immunotherapy, University of Michigan Rogel Cancer Center, University of Michigan School of Medicine, Ann Arbor, Michigan, USA.

[3]Department of Surgery, University of Michigan Rogel Cancer Center, University of Michigan School of Medicine, Ann Arbor, Michigan, USA.

[4]Department of Pathology, University of Michigan Rogel Cancer Center, University of Michigan School of Medicine, Ann Arbor, Michigan, USA.

[5]Department of Medical Oncology, University of Michigan Rogel Cancer Center, University of Michigan School of Medicine, Ann Arbor, Michigan, USA.

[6]Department of Periodontics and Oral Medicine, University of Michigan School of Dentistry, Ann Arbor, Michigan, USA

[7]Graduate Program in Immunology and Graduate Program in Cancer Biology, University of Michigan School of Medicine, Ann Arbor, Michigan, USA.

Abstract

Combinatorial strategies are needed to overcome the resistance of pancreatic cancer to immune checkpoint blockade (ICB). DNA damage activates the innate immune response and improves ICB efficacy. Since ATM is an apical kinase in the radiation-induced DNA damage response, we investigated the effects of ATM inhibition and radiation on pancreatic tumor immunogenicity. ATM was inhibited through pharmacologic and genetic strategies in human and murine pancreatic cancer models both in vitro and in vivo. Tumor immunogenicity was evaluated after ATM inhibition alone and in combination with radiation by assessing TBK1 and Type I Interferon (T1IFN) signaling as well as tumor growth following PD-L1/PD-1 checkpoint inhibition. Inhibition of ATM increased tumoral T1IFN expression in a cGAS/STING-independent, but TBK1 and SRC-dependent manner. The combination of ATM inhibition with radiation further enhanced TBK1 activity, T1IFN production, and antigen presentation. Furthermore, ATM

Correspondence: Meredith Morgan, PhD, Department of Radiation Oncology, University of Michigan, 1301 Catherine Street, 4326B Medical Sciences I, Ann Arbor, MI 48109. mmccrack@med.umich.edu, Phone: (734) 647-5928.

*, †These authors contributed equally to this work.

Conflict-of-interest disclosure: The authors declare no potential conflicts of interest.

silencing increased PD-L1 expression and increased the sensitivity of pancreatic tumors to PD-L1 blocking antibody in association with increased tumoral $CD8^+$ T cells and established immune memory. In patient pancreatic tumors, low ATM expression inversely correlated with PD-L1 expression. Taken together, these results demonstrate that the efficacy of ICB in pancreatic cancer is enhanced by ATM inhibition and further potentiated by radiation as a function of increased tumoral immunogenicity, underscoring the potential of ATM inhibition in combination with ICB and radiation as an efficacious treatment strategy for pancreatic cancer.

Keywords

Cancer; ATM; DNA Damage Response; Ionizing Radiation; Immunity; Immune Checkpoint Blockade; Interferon; PD-L1; Pancreatic Cancer

INTRODUCTION

Inhibition of the immune checkpoint through strategies such as PD-L1 and PD-1 blocking antibodies has emerged as a powerful oncologic treatment modality capable of producing durable responses in many cancer histologies (1). Pancreatic adenocarcinoma, however, is refractory to ICB therapy, likely due to limited $CD8^+$ effector T cell infiltration and activation (2). To improve the efficacy of ICB therapy in pancreatic cancer, differential combinatorial therapeutic strategies to enhance tumor immunogenicity as well as the intratumoral T cell number and function are needed.

Ionizing radiation can improve ICB efficacy through activation of multiple pathogen recognition receptors (PRR), which converge on TANK Binding Kinase 1 (TBK1), resulting in increased tumoral Type I interferon (T1IFN) production and subsequently enhanced innate and adaptive immune responses (3–6). Prior studies suggest that radiation activates TBK1 through the generation of DNA damage resulting in the release of single- or double-stranded DNA or micronuclei into the cytoplasm of cells (4,7). Cytoplasmic DNA is in turn sensed by anti-viral PRRs and their associated adapter proteins such as cGAS and STING, respectively, leading to activation of TBK1. TBK1 integrates signals from multiple PRRs leading to induction of T1IFN transcription and activation of innate immunity.

Interferon signaling plays pleotropic roles in the tumor microenvironment. Acute T1IFN production from tumor cells and plasmacytoid dendritic cells activates a coordinated anti-viral inflammatory response which increases tumor immune surveillance (8). The increased immune surveillance in response to T1IFN arises from its effects on the immune system such as the maturation of and antigen presentation by dendritic cells, activation of memory $CD8^+$ T cells, and inactivation of regulatory T cells (9). Emerging evidence also suggests, however, that chronic T1IFN production can lead to negative feedback mechanisms designed to limit immunopathology (10). Combinatorial strategies to reinvigorate anti-tumoral immune responses by enhancing immunogenic PRR signaling and promoting T1IFN production while simultaneously addressing negative feedback mechanisms are sought (11).

Defects in DNA damage response (DDR) proteins such as RAD51, RPA, and MUS81 can increase T1IFN production via the generation of cytoplasmic DNA (12–14). Ataxia

Telangiectasia Mutated (ATM) is an apical kinase in the DDR that plays a critical role in response to ionizing radiation-induced DNA double-strand breaks. Clinically, ATM mutations result in Ataxia-Telangiectasia (A-T), a syndrome marked by exquisite sensitivity to radiation, immune phenotypes, and inflammatory manifestations (15). Interestingly, A-T patients have altered innate immunity and increased interferon signaling resulting in enhanced anti-viral immunity (16). Furthermore, ATM loss results in the generation of cytoplasmic DNA and activation of cGAS/STING/TBK1. In contrast, ATM can promote a non-canonical, cGAS-independent innate immune response to etoposide-induced nuclear DNA damage (17,18). The role of ATM, however, in radiation-induced tumor innate immunity and T1IFN production is unknown

While we and others have shown the critical importance of the DDR including ATM in the growth and survival of pancreatic cancers following radiation (19,20), the contribution of the innate immune signaling axis to this response is unknown. Given the limited efficacy of ICB in pancreatic cancers, in the current study we examined whether inhibition of the DDR could cooperate with radiation to enhance innate immune signaling and, more importantly, ICB therapy efficacy. When we found that ATM inhibition was unique in its ability to activate the TBK1/T1IFN pathway, we went on to determine the mechanisms as well as the consequences of ATM inhibition on tumor growth and therapeutic responses to PD-L1 blocking antibody and radiation.

MATERIALS AND METHODS

Reagents and Cell Lines

ATM inhibitor KU60019 was purchased from Cayman Chemical. ATR inhibitor (AZD6738), PARP inhibitor (olaparib) and WEE1 inhibitor (AZD1775) were from AstraZeneca. Small interference RNAs targeting human and murine ATM, SRC, TBK1 and p70S6K were purchased from Dharmacon. Anti-human IFNAR2 neutralization antibody was purchased from PDI Assay Science. The MAR1–5A3 monoclonal antibody that reacts with mouse IFNAR-1 (IFN alpha/beta receptor subunit 1) was purchased from InVivoMab. Human pancreatic cancer cell line Panc1 and murine pancreatic cancer cell line mT4 were grown in DMEM (Gibco/Invitrogen) + 10% fetal bovine serum (Hyclone) (FBS) + 100 units/ml penicillin +100 μg/ml streptomycin, while Capan1 cells were cultured in IMEM supplemented with 10% FBS, 100 units/ml penicillin, and 100 μg/ml streptomycin. Murine pancreatic cancer cells KPC2 were grown in RPMI-1640 with 10% FBS and 100 units/ml penicillin +100 μg/ml streptomycin. KPC2 (also known as 65.671) and mT4 cells were obtained through collaboration with Dr. Pasca di Magliano (University of Michigan) (21,22). Capan1 Neo cells were obtained from Dr. S. Powell (Memorial Sloan Kettering Cancer Center, New York, NY). Panc1 cells were obtained from ATCC. Cells were authenticated (via short tandem repeat profiling) by the ATCC and cryopreserved within 3 months of authentication. All cells were routinely screened for mycoplasma. mT4 cells were transfected with pCI-neo-mOVA plasmid by Lipofectamine 2000 (Invitrogen) according to the manufacturer’s instructions. The cells were selected with G418, and ovalbumin expression was confirmed by flow cytometry and used for in vitro antigen presentation assay.

Genetically Modified Cell Lines

STING or cGAS knockout cells were generated with CRISPR/Cas9 Technology. Panc1 or Capan1 cells were transduced with lenti-CRISPR lentiviral constructs encoding Cas9 and the control, STING or cGAS guide RNAs. Positive cells were selected by adding puromycin (2μg/ml) at 48 hours after lentiviral infection. Single-cell clones were selected and expanded. ATM silenced murine and human pancreatic cancer cell lines were generated by infecting the cells with sh-control or shATM virus (pLenti-CMV-Puro-Luciferase). The cells were then selected with puromycin to generate stable cell lines.

Western Blotting

Western blotting was performed as described (23,24). Whole-cell extract was prepared by sonicating cells in a sodium dodecyl sulfate (SDS) sample buffer containing protease inhibitor and phosphatase inhibitor. After boiling at 95°C for 10 minutes, samples were separated by SDS-PAGE and transferred to polyvinylidene fluoride (PVDF) membranes (Millipore). The following primary antibodies were used in this study: anti-TBK1 (D1B4), anti-p-TBK1 (S172, D52C2), anti-STAT1 (Y701, D4Y6Z), anti-p-STAT1 (58D6), ATM (D2E2), anti-STING (D2P2F), anti-human cGAS (D1D3G), anti-mouse cGas (D3O8O), anti-SRC (36D10), anti-p-SRC (Y416, D49G4), anti-p-CHK2 (T68), anti-p70 S6K (49D7), anti-p-S6K (108D2) (Cell Signaling), anti-mouse Pd-l1 (MAB90781, R&D Systems), and anti-CHK2 (05–649, Millipore).

Human Phospho-Kinase Antibody Array

The Human Phospho-Kinase Array Kit (#ARY003B) was purchased from R&D Systems. Array screening was performed following the manufacturer's protocol. Briefly, Panc1 cell lysates treated with DMSO or ATM inhibitor KU60019 (3 hr) were incubated with the array membranes. After washing, the membranes were incubated with biotinylated antibody cocktail. The amounts of phospho-kinase were assessed with streptavidin conjugated to horseradish peroxidase (HRP), followed by chemiluminescence detection. The Image J software was used to quantify the density of each dot against the average of the internal controls on the membrane.

IFNB1–GFP Reporter Assay

Type I interferon was measured using a reporter promotor plasmid as previously described (7). Briefly, pIFNB1-GFP reporter containing *IFNB1* promoter was stably transfected into Panc1 cells and positive cells were selected with 50 μg/mL hygromycin. Upon ATM inhibitor and/or radiation treatment, expression of GFP was analyzed by flow cytometry. After extraction of background GFP expression (baseline), the changed mean fluorescent intensity (MFI) for indicated treatments was determined.

Quantitative RT-PCR

Total RNA was isolated from cells by column purification (Direct-zol RNA Miniprep Kit, Zymo Research) with DNase treatment. cDNA was synthesized using High-Capacity cDNA Reverse Transcription Kit (Thermo Fisher Scientific) with poly-dT or random hexamer primers. Quantitative PCR (qPCR) was performed on cDNA using Fast SYBR® Green

Master Mix (Thermo Fisher Scientific) on a StepOnePlus™ Real-Time PCR System (Thermo Fisher Scientific). Fold changes in mRNA expression were calculated by the ΔΔCt method using GAPDH or ACTB as an endogenous control. All fold changes are expressed normalized to the untreated control.

Immunohistochemical Staining

Paraffin embedded pancreatic tumor tissue microarrays were prepared as previously described (25). The slides were baked for 60 minutes at 60 °C and then deparaffinized in xylene and rehydrated through graded concentrations of ethanol in water. The slides were then subjected to antigen retrieval in 1X AR6 or AR9 buffer (PerkinElmer) using microwave treatment. IHC staining was performed using EnVision G|2 Doublestain System (Agilent) and with conditions for ATM staining (Y170, ab32420; Abcam) that were previously described (26). Sections were left to air-dry and mounted with permanent mounting medium and coverslipped. Bright field images were acquired by an automated slide-scanning platform (Aperio AT2, Leica Biosytems) at a 400× magnification. The images were analyzed with ImageScope software (Leica Biosystems). The tissue cores were scored manually using a light microscope by diagnostic pathologists. The tumoral ATM level in each core (1 mm2) was determined by the H-score method. The H score method takes the percentage of positive cells (0 –100%) and each staining intensity (0 – 3+, negative - strong) into account where the H-score = (% positive) × (intensity). Cores from normal skin tissue of scalp, abdominal part and breast were used as controls.

Multiplex Fluorescent Immunohistochemistry (mfIHC)

The TMAs, previously mentioned, were subject to mfIHC. After deparffinization and rehydration with xylene and ethanol, the TMAs was subject to multiple rounds of antigen retrieval with AR6 or AR9 (Akoya Biosciences). Primary and secondary antibody application was followed by Opal tyramide signal amplification (Akoya Biosciences), as described (27). The following antibodies were used to evaluate the immune and cancer cell populations: pancytokeratin (Dako, A0452, 1:400), PD-L1 (Cell Signaling, 13684, 1:200), CD163 (Lecia, NCL-L-CD163, 1:400), and Spectral DAPI (Akoya Biosciences). After staining and mounting with Prolong Diamond (Thermofisher), images of each core were captured using the Mantra™ Quantitative Pathology Workstation (Akoya Biosciences).

Analysis of mfIHC and IHC

Images captured by the Mantra™ Quantitative Pathology Workstation (Akoya Biosciences) were uploaded into the inForm software program (Akoya Biosciences). Cells were phenotyped using inForm, as previously described (27). The H-score for each core of the IHC treated TMAs were matched to the corresponding cores for the duplicate TMAs that underwent mfIHC. PD-L1 positivity of both the APCs and epithelial cells were divided into two groups: low and high using quartiles. The ATM H-score was then compared in each group.

In Vivo Mouse Models

10– to 12-week-old NOD.Cg-Prkdcscid Il2rgtm1Wjl/SzJ (NSG) mice and wild type C57BL/6 and FVB/NJ mice were obtained from the Jackson Laboratory. mT4 pancreatic cancer cells (10^6) were subcutaneously injected to the right flank of female C657BL/6 or NSG mice. KPC2 pancreatic cancer cells (10^6) were subcutaneously injected to the right flank of female FVB/NJ or NSG mice. Anti–PD-L1 and IgG1 isotype control were given intraperitoneally 100 ug/mouse every 3 days after tumors reached approximately 75 mm^3. A single fraction of 8 Gy was given when tumors reached ~100–150 mm^3. Tumor diameters were measured using calipers. All animal procedures were approved by the IACUC Committee of the University of Michigan.

Flow Cytometry Analysis

Single cell suspensions of bone marrow derived macrophages or mT4-Ova tumor cells were analyzed by flow with antibodies recognizing Ova257–264 (SIINFEKL) bound to H-2Kb of MHC class I (Invitrogen, 25-D1.16) or H-2Kb of MHC class I (Invitrogen, AF6–88.5.5.3). To analyze CD8 T cell activity, single-cell suspensions were prepared from fresh mouse tissues. Cell suspensions were then overlaid on ficoll and lymphocytes were obtained by density gradient centrifuge. For cytokine staining, lymphocytes were incubated with PMA (5ng/ml), Ionomycin (500 ng/ml), Brefeldin A (1: 1000) and Monensin (1: 1000), 4 hours in a 37°C CO_2 incubator. Anti-CD45, anti-CD90, anti-CD4 and anti-CD8 were added for 20 minute for surface staining. The cells were then washed and suspended in 1 ml of freshly prepared Permeabilization Buffer A and B, and incubated at 4°C overnight. Cells were washed and stained for intracellular cytokine expression.

Gene Correlation Analysis

ATM correlation analysis in TCGA datasets in R. The ATM loss, SRC, and interferon response gene signatures were defined as previously described (28–30). The ATM loss signature was cross-validated for ATM loss in the pancreas using GSEA (31).

Statistical and Patient Survival Analyses

GraphPad Prism6 software (GraphPad Software, Inc.) was used for statistical analysis. The two-tailed paired student’s t-test or one-way ANOVA was employed to verify whether the difference between groups were statistically significant. P-values < 0.05 were considered to be statistically significant.

RESULTS

ATM inhibition enhances the Type I Interferon signaling pathway via TBK1 activation

It is unknown whether pharmacologic inhibition of the DDR can induce T1IFN and tumor immunity. To test the hypothesis that pharmacologic inhibition of the DDR activates innate immune pathways leading to T1IFN production, we treated human pancreatic cancer cells with a panel of DDR targeting agents. Although inhibitors of ATR, PARP1, or WEE1, had minimal effect, we found that inhibition of ATM by KU60019 caused a concentration-dependent increase in phosphorylation of both TBK1 and STAT1 (Fig. 1A) under conditions

that selectively inhibited ATM relative to other phosphoinositide 3-kinases (Supp. Fig. 1A). ATM inhibition increased TBK1 and STAT1 phosphorylation in a panel of human and murine pancreatic cancer models including Capan1, KPC2, and mT4, respectively, and in association with a decrease in the ATM substrate pCHK2 (Fig. 1B–D, Suppl. Fig. 1 B, C). To genetically assess TBK1 phosphorylation in response to ATM inhibition, we inhibited ATM using siRNA. Silencing of ATM in pancreatic cell lines resulted in increased phosphorylation of TBK1 and STAT1 (Fig. 1E–H, Suppl. Fig. 1D, E). To extend these findings to ATM mutant models, we next examined fibroblasts derived from A-T patients in which ATM is mutated and catalytically inactive or reconstituted with wild type ATM. We found that A-T fibroblasts also displayed increased TBK1 and STAT1 phosphorylation (Suppl. Fig. 1F), demonstrating that ATM regulates innate immune signaling in a variety of cellular contexts.

A consequence of TBK1 mediated innate immune sensing is T1IFN production (32). To determine whether ATM inhibition affected T1IFN production, Panc1 cells stably expressing a fluorescent *IFNB1* promoter reporter (7) were treated with ATM inhibitor or siRNA, which resulted in a concentration dependent increase in T1IFN reporter activity (Fig. 1I, J). In agreement, we found that *Ifna2* mRNA levels were elevated in response to ATM inhibition in KPC2 cells (Fig. 1K). Consistent with the requirement for TBK1 in T1IFN production, induction of the T1IFN reporter in response to ATM inhibition was dependent on TBK1 as siRNA-mediated depletion of TBK1 significantly inhibited T1IFN reporter activity (Fig. 1L).

To determine whether ATM inhibition induced phosphorylation of STAT1 through TBK1 and subsequent autocrine T1IFN signaling, we treated Panc1 cells with ATM inhibitor or siRNA and IFNAR blocking antibody. We observed abrogation of STAT1 phosphorylation, but, as expected, not TBK1 phosphorylation (Fig. 1M, N, Suppl. Fig. 1G). To assess the clinical relevance of this finding, we first defined an ATM loss gene signature by querying previously published microarray data of ATM expression loss in pancreatic tumors (33). We next queried the gene expression profile in tumors from pancreatic cancer patients in the TCGA cohort (34). We found a positive correlation between the ATM loss and interferon response signatures (Fig. 1O). Together, these data suggest that ATM constrains T1IFN signaling, and establishes that pharmacologic inhibition of ATM may be a novel therapeutic strategy to modulate T1IFN signaling in pancreatic cancer.

ATM inhibition activates TBK1 in a cGAS/STING-independent manner

The nucleic acid sensor cGAS and its adapter STING have been implicated in the activation of TBK1 in response to radiation and some DDR defects (3,12,35). Given that both cGAS and STING were abundantly expressed in pancreatic cancer cells (Suppl. Fig. 2A), we assessed the requirement for both cGAS and STING in activation of TBK1 following ATM inhibition with CRISPR/Cas9-mediated STING or cGAS-deleted Panc1 and Capan1 cells. Although the basal level of pTBK1 was increased in STING-deleted cells, neither STING nor cGAS deletion affected the induction of pTBK1 or pSTAT1 in response to ATM siRNA or KU60019 suggesting a cGAS/STING-independent mechanism (Fig. 2A, B; Suppl. Fig. 2B–D). To characterize this mechanism, we examined the kinetics of TBK1 and STAT1

activation in response to ATM inhibitor. Treatment of Panc1 or mT4 cells with ATM inhibitor resulted in rapid TBK1 phosphorylation (1 hour) followed by increased STAT1 phosphorylation (6 hours) (Fig. 2C, Suppl. Fig. 2E).

Since ATM is a pleiotropic kinase, we hypothesized that ATM inhibition may be affecting signal transduction pathways upstream of TBK1. Phospho-proteomic profiling of Panc1 cells treated with ATM inhibitor revealed reduced phosphorylation of known ATM targets CHK2 and AKT2 in addition to increased phosphorylation of P70-S6K and SRC (Fig. 2D). Neither pharmacologic (LY2584702) nor genetic (siRNA) inhibition of P70-S6K altered the ability of ATM inhibitor to induce TBK1 phosphorylation (Suppl. Fig. 2F, G).

As SRC regulates the crosslinking of multiple PRRs with TBK1 to promote T1IFN production in response to viral infections (36), we next assessed whether SRC was required for phosphorylation of TBK1 in response to ATM inhibition. Following confirmation of activating phosphorylation (Y419) of SRC by genetic inhibition of ATM (Fig. 2E, Suppl. Fig. 2H), we found that while pSRC was not detectable at baseline, pSRC was rapidly increased in response to ATM inhibition with similar kinetics to TBK1 phosphorylation (Suppl. Fig. 2I, J). Genetic silencing of SRC, in contrast to STING silencing, abrogated the induction of TBK1 phosphorylation in response to ATM inhibitor (Fig. 2F). Furthermore, SRC silencing prevented *IFNB1* reporter activation following ATM inhibition (Fig. 2G, Suppl. Fig. 2K). In addition, pharmacologic inhibition of SRC attenuated *IFNB1* reporter activity in Panc1 cells treated with ATM inhibitor (Suppl. Fig. 2L). To assess the clinical relevance of SRC signaling in pancreatic cancer, we examined gene expression profiles of pancreatic cancers from the TCGA database and found a significant positive correlation between the ATM loss gene signature and a previously validated SRC activity gene signature (Fig. 2H). Taken together, these data demonstrate that ATM inhibition causes TBK1 activation and T1IFN production in a STING-independent manner via regulation of SRC.

ATM inhibition cooperates with radiation to enhance TBK1 activation and Type I interferon signaling

ATM inhibition synergizes with radiation to promote tumor cell death by preventing the repair of radiation-induced DNA double strand breaks (37). We wished to determine whether ATM inhibition and radiation also cooperate to promote an innate immune response via the T1IFN pathway. Human and murine pancreatic cancer cells treated with ATM inhibitor and radiation were assessed for pTBK1 and pSTAT1 at 6 days after 20Gy, a radiation dose and time point selected based on its ability to generate cytoplasmic DNA (i.e. micronuclei) and a STAT1 response (7). We found that while ATM inhibitor or radiation alone induced TBK1 and STAT1 phosphorylation, that the combination had a greater effect than either agent alone (Fig. 3A, B, Suppl. Fig. 3A, B) resulting in 6–38-fold and 6–13-fold increases in pTBK1 and pSTAT1, respectively, relative to baseline across the 4 cell lines (Fig. 3C, D). Genetic inhibition of ATM in combination with radiation also caused a robust increase in TBK1 and STAT1 phosphorylation. (Fig. 3E, Suppl. Fig. 3C).

Both ablative and moderately hypofractionated radiation doses increase T1IFN production (4,7). To assess the dose dependency of radiation in combination with ATM inhibition, we assessed TBK1 and STAT1 activation in response to 8Gy. Consistent with the effects

observed at 20Gy (Fig. 3A), we found that 8Gy in combination with ATM inhibitor activated TBK1 and STAT1 signaling (Suppl. Fig 3C). We next investigated the combined effect of ATM inhibition and radiation on the activity of the human *IFNB1* reporter. As previously reported (4,5), radiation induced T1IFN production (Fig. 3F, G). More importantly, both genetic and pharmacologic inhibition of ATM further enhanced radiation-induced T1IFN reporter activity (Fig. 3F, G) and *Ifna2* expression (Suppl. Fig. 3D). Consistent with the role of SRC-dependent effects of ATM inhibition on TBK1, we found that T1IFN expression was impaired by either SRC inhibition (Suppl. Fig. 3E) or TBK1 silencing (Suppl. Fig. 3F).

To functionally define the consequence of ATM inhibition and radiation *in vitro*, we collected media from mT4 cells that had been silenced for ATM using short hairpin RNA and/or treated with radiation (Suppl. Fig. 3G), and subsequently transferred this conditioned media to murine bone marrow derived macrophages and measured the extracellular expression of the classical interferon response gene MHCI. While media from ATM silenced or radiation treated mT4 cells slightly increased MHCI expression, the combination strongly increased MHCI expression (Fig. 3H). Moreover, this increase could be blocked by the addition of IFNAR1 blocking antibody. T1IFN can also lead to increased expression of antigen presentation molecules such as MHCI on tumor cells. To assess the functional consequence of ATM inhibition on antigen presentation, we transduced murine pancreatic adenocarcinoma cell lines with ovalbumin and examined the extracellular expression of MHCI loaded with the modal antigen SIINFEKL (Ova). ATM silencing resulted in increased MHCI-Ova complexes, an effect that was further enhanced by treatment with radiation (Fig. 3I). To confirm that antigen presentation was enhanced secondary to T1IFN production, we pretreated cells with IFNAR blocking antibody which diminished induction of MHCI-Ova in response to ATM inhibition and radiation (Fig. 3J). Finally, we investigated the clinical relevance of this relationship between ATM and MHCI by querying its relevance in the pancreatic TCGA cohort. We found a significant positive correlation between an ATM loss signature and MHCI expression in human pancreatic tumors (Fig. 3K). Taken together, these data highlight that ATM inhibition and ionizing radiation cooperate to activate T1IFN transcription leading to enhanced antigenicity of pancreatic cancers that may in turn promote enhanced tumor immunity.

ATM inhibition increases pancreatic tumor immunity and sensitizes to immune checkpoint blockade *in vivo*

To examine the potential role of ATM in tumor immunity *in vivo*, Atm wild type or Atm silenced mT4 or KPC2 cells were implanted into either syngeneic immunocompetent or immunodeficient mice. Consistent with a previously characterized Atm deleted autochthonous pancreatic cancer model (33), we found that Atm silencing resulted in a modest growth advantage of KPC2 tumors in immunocompetent mice (FVB/NJ, Fig. 4A). Surprisingly, this enhanced growth of Atm deficient KPC2 tumors was dependent on an intact immune system as the effect was absent in NOD.SCID γc-deficient (NSG) mice (Fig. 4B). To confirm this finding, we conducted similar experiments in Atm wild type or Atm silenced mT4 pancreatic tumors in wild type or NSG mice. Again, we found an immune dependent growth advantage of Atm deficient tumors (Fig. 4C, D).

Given that PD-L1 is an interferon response gene (38), interferon production in response to loss of ATM may promote the activation of the PD-L1/PD-1 immune checkpoint (10). Therefore, we examined Pd-l1 expression following silencing of Atm in KPC2 and mT4 cells and found increased Pd-l1 expression in response to Atm silencing both in pancreatic cancer cells and tumors *in vivo* (Suppl. Fig. 4A, Fig. 4E), a finding that is distinct from the reported requirement for ATM in PD-L1 expression (39). In addition, and consistent with our *in vitro* results, Atm silenced tumors had increased phosphorylation of Src, Tbk1, and Stat1 (Fig. 4E). Consistent with increased Stat1 activation and tumoral production of T1IFN, we observed that tumoral macrophages expressed a $MHCII^{+}CD80^{+}$ pro-inflammatory phenotype (Fig. 4F). We hypothesized that the increased Pd-l1 expression in Atm silenced tumors would lead to activation of the Pd-l1/Pd-1 immune checkpoint and consequently increased sensitivity to Pd-l1/Pd-1 checkpoint blockade therapy. To test whether Atm deficient tumors were more sensitive to inhibition of the Pd-l1/Pd-1 immune checkpoint, Atm wild type or silenced mT4 cells were implanted into $Pd1^{-/-}$ mice. In contrast to Atm wild type tumors, Atm silenced tumors exhibited markedly slower tumor growth in $Pd1^{-/-}$ deficient mice and underwent spontaneous rejection (Fig. 4G).

The finding that Pd-l1 is increased in Atm silenced tumors, suggested that Pd-l1 may represent a therapeutically actionable vulnerability in these tumors. Furthermore, since radiation also stimulates innate immunity and immune checkpoint therapy efficacy, we initiated studies to compare the effectiveness of combined radiation and anti-PD-L1 therapy. While treatment with Pd-l1 antibody did not slow the growth of control tumors (Fig. 4H), Pd-l1 antibody did inhibit the growth of Atm silenced tumors (Fig. 4I). Furthermore, radiation in combination with Pd-l1 antibody further inhibited the growth of Atm deficient tumors relative to control tumors, producing cures in 100% of the Atm silenced tumors and 0% of the control tumors. To confirm this dramatic response, we conducted similar studies with Atm silenced KPC2 tumors implanted in syngeneic FVB mice. Similar to the observed effects in mT4 tumors, Atm silenced KPC2 tumors were more sensitive to Pd-l1 antibody with the most dramatic growth inhibition occurring in Atm silenced tumors treated with the combination of PD-L1 antibody and radiation (Fig. 4J, K). Taken together these results demonstrate that increased interferon signaling and innate immunity in Atm deficient tumors promotes sensitivity to Pd-l1/Pd-1 immune checkpoint blockade that is further enhanced by radiation.

T1IFN production can enhance the production of T cell recruiting chemokines (23). To assess whether radiation and PD-L1 antibody interact with ATM genetic status to promote T cell migration, we quantified intratumoral $CD8^{+}$ T cells. Interestingly, we observed that Atm silenced tumors had increased $CD8^{+}$ T cells as compared to control tumors (Fig. 4L, Suppl. Fig. 4B). Furthermore, radiation and PD-L1 antibody cooperatively promoted tumoral T cell trafficking only in Atm silenced tumors. To understand if Atm loss combined with radiation and PD-L1 blocking antibody could systemically alter adaptive immunity, immunophenotyping was performed on spleens from tumor bearing mice. We observed that in mice bearing Atm silenced tumors, the combination of Pd-l1 antibody and radiation more strongly increased $CD8^{+}$ T cell proliferation, and production of IFN-γ and Granzyme B relative to Atm wild type tumors (Suppl. Fig. 4C–E). To functionally confirm that Atm silenced tumors treated with Pd-l1 antibody and radiation resulted in adaptive immunologic

memory, tumor naïve or previously cured mice (Fig. 4I) were inoculated with Atm silenced mT4 tumors. In support of an established T cell memory, previously cured mice rejected Atm silenced mT4 cells, while tumor naïve mice had 100% tumor engraftment rates (Fig. 4M). Finally, we wished to extend these findings to human pancreatic adenocarcinomas. Using a tissue microarray of pancreatic neoplasms, we observed that ATM expression was retained in 96.7% of normal and premalignant neoplasms, but was reduced in 25.9% of primary pancreatic adenocarcinomas. We observed that both tumoral and antigen presenting cell expression of PD-L1 was increased in tumors expressing low levels of ATM (Fig. 4N, O; Suppl. Fig. 4F). Taken together, these data demonstrate that ATM regulates the growth of pancreatic tumors in an immune dependent manner. Loss of ATM expression causes an increase in PD-L1 expression, a finding that is recapitulated in human pancreatic cancers with low ATM expression. Importantly, Pd-l1 expression in ATM silenced tumors leads to enhanced sensitivity to therapy with Pd-l1 blocking antibody that is further potentiated by combined treatment with radiation. These results suggest that ATM inhibition causes engagement of an immune checkpoint rendering tumors highly sensitive to combined immune checkpoint and radiation therapy.

DISCUSSION

In this study, we have found that ATM regulates interferon signaling in pancreatic cancer such that ATM inhibition induces TBK1 activation and T1IFN production that is further enhanced by radiation. Mechanistically, our data support a model in which SRC is a key regulator in the TBK1 and T1IFN response following ATM inhibition (Suppl. Fig. 4G). *In vivo*, the consequence of ATM silencing is increased interferon signaling as well as increased PD-L1 expression. Consequently, ATM deficient tumors are sensitized to combination therapy with PD-L1 blockade and radiation. The regulation of interferon signaling by ATM represents a connection between the DDR and innate immunity that can be exploited to enhance the efficacy of ICB therapy in otherwise resistant pancreatic cancers.

Significant interest has been placed in activating innate immunity to enhance ICB efficacy. Radiation activates innate immune signaling via the induction of DNA damage leading to release of damaged DNA into the cytoplasm either via circumventing the DNA exonuclease Trex1 or mitotic mis-segregation of radiation-damaged acentric chromosomes leading to the generation of micronuclei (4,7). Cytoplasmic DNA induces the cGAS/STING pathway leading to TBK1 activation and T1IFN production. Given the importance of DNA damage and the DDR to interferon signaling, DDR inhibitors are under investigation in the context of immune-oncology. For example, PARP inhibitors enhance the efficacy PD-L1 inhibitors through mechanisms involving PD-L1 upregulation (40) and activation of cGAS/STING innate immune signaling (41). ATR inhibitors reduce radiation-induced PD-L1 expression and thus activate $CD8^+$ T cell activity and attenuate T cell exhaustion (42). In contrast, DNAPK inhibition may limit innate immunity in p53 wild type cells by preventing the mitotic division and therefor the generation of immunogenic micronuclei (7). Relative to these studies, we demonstrate for the first time ATM as an important target for pharmacologic modulation of innate immune signaling and consequently sensitivity to ICB therapy.

ATM inhibitors have been developed with the goal of sensitizing tumors DNA damage induced by radiation or chemotherapy. There are currently multiple ATM inhibitors in clinical development such as M3541 and AZD0156 with early trials focused on their combinations with chemotherapy (e.g., irinotecan) or radiation. The findings in this paper highlight that ATM inhibition may also be able to sensitize to ICB and specifically PD-L1 inhibitors by their ability to induce tumoral interferon signaling. As the ratio of tumor burden to T cell activation dictates the success of ICB therapy (43), this work suggests that ATM inhibition, radiation, and ICB may be a novel rational therapeutic combination to improve clinical outcomes in pancreatic cancer. It will be important in future studies to assess the effects of pharmacologic ATM inhibitors in autochthonous pancreatic tumor models which more closely mimic the inhibitory immune environment of human pancreatic tumors.

Another potential therapeutic implication of this study is that loss of ATM expression or function by inactivating mutation may confer increased sensitivity to ICB. While defects in ATM occur in a significant minority of pancreatic cancers (10–20%), recently ATM mutations were found to be a defining characteristic of an ‘immune rich’ subtype of human pancreatic tumors associated with improved patient outcomes (33,44). Similarly, we found that reduced expression of ATM correlated with PD-L1 expression in pancreatic cancer patients. Therefore, it is important to evaluate whether ICB has therapeutic efficacy in patients with ATM deficient tumors, especially those treated with radiation therapy. Furthermore, other cancers such as lung adenocarcinoma (26) may have a much higher prevalence of ATM loss/mutation (40%) underscoring the need for analysis of ICB efficacy in the context of ATM status in these cancers.

The cGAS/STING pathway has been implicated in the activation of innate immunity in response to DDR inhibition (41). While radiation-induced innate immune signaling depends on the cGAS/STING pathway (3,4), our study demonstrates that ATM regulates signaling to TBK1 independent of cGAS/STING (Fig. 2A, B). This is consistent with a model in which radiation activates the cGAS/STING pathway (via the generation of cytoplasmic DNA) while ATM regulates signal transduction mechanisms to increase the phosphorylation and activity of TBK1 and hence the innate immunity (Suppl. Fig. 4G). Our results show that ATM regulates SRC to modulate TBK1 and T1IFN, which is consistent with the role of SRC in promoting the formation of PRR complexes with TBK1 (36). This report highlights that ATM may restrain SRC activity to prevent excessive inflammatory signaling such that loss of ATM function results in SRC activation leading to enhanced formation of TBK1-PRR complexes and T1IFN production. It will be important in future studies to identify the PRRs downstream of ATM and SRC as well as to identify other signaling intermediaries.

Interferon signaling plays pleomorphic roles in the immune microenvironment (45,46). Loss of interferon signaling compromises anti-tumoral immunity, and patients with an interferon signature are more likely to clinically benefit from immune checkpoint (47). Low level interferon signaling can also promote tumor growth and adaptive resistance to immunotherapy (48). There is increasing recognition that T1IFN production by tumor cells contributes to radiotherapy and cytotoxic chemotherapy efficacy (49). This work highlights ATM inhibition as a novel strategy to increase tumoral T1IFN singling and subvert the

immunosuppressive networks in the tumor microenvironment to promote anti-tumoral immunity (50,51).

In conclusion, this study defines a novel direct link between the DDR and immunotherapy. There are important clinical implications of this work in the context of therapeutic strategies combining ATM inhibitors with ICB and radiation as well as using ATM loss/mutation as a potential marker of sensitivity to ICB. These approaches are especially important in the context of pancreatic cancer which to date has been resistant to all therapy including ICB. Our study supports the pre-clinical and subsequent clinical investigation of ATM inhibitors in combination radiation as a strategy to increase the immunogenicity of pancreatic tumors and sensitize them to ICB.

Supplementary Material

Refer to Web version on PubMed Central for supplementary material.

Support:

This work was supported by the Janet Binder Robinson and Samuel Binder Pancreatic Cancer Research Funds, the Roger and Gloria DeMeritt Pancreatic Cancer Research Funds (MM), U01CA216440 (TL), Cancer Center Support Grant P30CA46592, and in part by CA123088, CA099985, CA156685, CA171306, CA190176, CA193136, CA211016, 5P30CA46592 (WZ), DE026728 (YL), and CA234222 (JS).

REFERENCES

1. Zou W, Wolchok JD, Chen L. PD-L1 (B7-H1) and PD-1 pathway blockade for cancer therapy: Mechanisms, response biomarkers, and combinations. Sci Transl Med 2016;8(328):328rv4 doi 10.1126/scitranslmed.aad7118.
2. Brahmer JR, Tykodi SS, Chow LQ, Hwu WJ, Topalian SL, Hwu P, et al. Safety and activity of anti-PD-L1 antibody in patients with advanced cancer. The New England journal of medicine 2012;366(26):2455–65 doi 10.1056/NEJMoa1200694. [PubMed: 22658128]
3. Deng L, Liang H, Xu M, Yang X, Burnette B, Arina A, et al. STING-Dependent Cytosolic DNA Sensing Promotes Radiation-Induced Type I Interferon-Dependent Antitumor Immunity in Immunogenic Tumors. Immunity 2014;41(5):843–52 doi 10.1016/j.immuni.2014.10.019. [PubMed: 25517616]
4. Vanpouille-Box C, Alard A, Aryankalayil MJ, Sarfraz Y, Diamond JM, Schneider RJ, et al. DNA exonuclease Trex1 regulates radiotherapy-induced tumour immunogenicity. Nature communications 2017;8:15618 doi 10.1038/ncomms15618.
5. Burnette BC, Liang H, Lee Y, Chlewicki L, Khodarev NN, Weichselbaum RR, et al. The efficacy of radiotherapy relies upon induction of type i interferon-dependent innate and adaptive immunity. Cancer Res 2011;71(7):2488–96 doi 10.1158/0008-5472.CAN-10-2820. [PubMed: 21300764]
6. Yoneyama M, Kikuchi M, Natsukawa T, Shinobu N, Imaizumi T, Miyagishi M, et al. The RNA helicase RIG-I has an essential function in double-stranded RNA-induced innate antiviral responses. Nature Immunology 2004;5:730 doi 10.1038/ni1087. [PubMed: 15208624]
7. Harding SM, Benci JL, Irianto J, Discher DE, Minn AJ, Greenberg RA. Mitotic progression following DNA damage enables pattern recognition within micronuclei. Nature 2017;548(7668): 466–70 doi 10.1038/nature23470. [PubMed: 28759889]
8. Purbey PK, Scumpia PO, Kim PJ, Tong A-J, Iwamoto KS, McBride WH, et al. Defined Sensing Mechanisms and Signaling Pathways Contribute to the Global Inflammatory Gene Expression Output Elicited by Ionizing Radiation. Immunity 2017;47(3):421–34.e3. [PubMed: 28930658]
9. Zitvogel L, Galluzzi L, Kepp O, Smyth MJ, Kroemer G. Type I interferons in anticancer immunity. Nature Reviews Immunology 2015;15(7):405.

10. Patel SA, Minn AJ. Combination Cancer Therapy with Immune Checkpoint Blockade: Mechanisms and Strategies. Immunity 2018;48(3):417–33 doi 10.1016/j.immuni.2018.03.007. [PubMed: 29562193]
11. Yang X, Zhang X, Fu ML, Weichselbaum RR, Gajewski TF, Guo Y, et al. Targeting the tumor microenvironment with interferon-beta bridges innate and adaptive immune responses. Cancer cell 2014;25(1):37–48 doi 10.1016/j.ccr.2013.12.004. [PubMed: 24434209]
12. Ho SS, Zhang WY, Tan NY, Khatoo M, Suter MA, Tripathi S, et al. The DNA Structure-Specific Endonuclease MUS81 Mediates DNA Sensor STING-Dependent Host Rejection of Prostate Cancer Cells. Immunity 2016;44(5):1177–89 doi 10.1016/j.immuni.2016.04.010. [PubMed: 27178469]
13. Wolf C, Rapp A, Berndt N, Staroske W, Schuster M, Dobrick-Mattheuer M, et al. RPA and Rad51 constitute a cell intrinsic mechanism to protect the cytosol from self DNA. Nature communications 2016;7:11752 doi 10.1038/ncomms11752.
14. Mouw KW, Goldberg MS, Konstantinopoulos PA, D'Andrea AD. DNA Damage and Repair Biomarkers of Immunotherapy Response. Cancer Discov 2017;7(7):675–93 doi 10.1158/2159-8290.CD-17-0226. [PubMed: 28630051]
15. Lavin MF, Shiloh Y. THE GENETIC DEFECT IN ATAXIA-TELANGIECTASIA. Annual Review of Immunology 1997;15(1):177–202 doi 10.1146/annurev.immunol.15.1.177.
16. Hartlova A, Erttmann SF, Raffi FA, Schmalz AM, Resch U, Anugula S, et al. DNA damage primes the type I interferon system via the cytosolic DNA sensor STING to promote anti-microbial innate immunity. Immunity 2015;42(2):332–43 doi 10.1016/j.immuni.2015.01.012. [PubMed: 25692705]
17. Dunphy G, Flannery SM, Almine JF, Connolly DJ, Paulus C, Jonsson KL, et al. Non-canonical Activation of the DNA Sensing Adaptor STING by ATM and IFI16 Mediates NF-kappaB Signaling after Nuclear DNA Damage. Mol Cell 2018;71(5):745–60 e5 doi 10.1016/j.molcel.2018.07.034. [PubMed: 30193098]
18. Brzostek-Racine S, Gordon C, Van Scoy S, Reich NC. The DNA damage response induces IFN. J Immunol 2011;187(10):5336–45 doi 10.4049/jimmunol.1100040. [PubMed: 22013119]
19. Morgan MA, Lawrence TS. Molecular Pathways: Overcoming Radiation Resistance by Targeting DNA Damage Response Pathways. Clinical cancer research: an official journal of the American Association for Cancer Research 2015;21(13):2898–904 doi 10.1158/1078-0432.CCR-13-3229.
20. Ayars M, Eshleman J, Goggins M. Susceptibility of ATM-deficient pancreatic cancer cells to radiation. Cell Cycle 2017;16(10):991–8 doi 10.1080/15384101.2017.1312236. [PubMed: 28453388]
21. Zhang Y, Morris JPt, Yan W, Schofield HK, Gurney A, Simeone DM, et al. Canonical wnt signaling is required for pancreatic carcinogenesis. Cancer Res 2013;73(15):4909–22 doi 10.1158/0008-5472.CAN-12-4384. [PubMed: 23761328]
22. Boj SF, Hwang CI, Baker LA, Chio II, Engle DD, Corbo V, et al. Organoid models of human and mouse ductal pancreatic cancer. Cell 2015;160(1–2):324–38 doi 10.1016/j.cell.2014.12.021. [PubMed: 25557080]
23. Peng D, Kryczek I, Nagarsheth N, Zhao L, Wei S, Wang W, et al. Epigenetic silencing of Th1 type chemokines shapes tumor immunity and immunotherapy. Nature 2015;527(7577):249. [PubMed: 26503055]
24. Wang W, Kryczek I, Dostál L, Lin H, Tan L, Zhao L, et al. Effector T Cells Abrogate Stroma-Mediated Chemoresistance in Ovarian Cancer. Cell 2016;165(5):1092–105 doi 10.1016/j.cell.2016.04.009. [PubMed: 27133165]
25. Shankar S, Tien J, Siebenaler RF, Dommeti VL, Zelenka-Wang S, Juckette KM, et al. An Essential Role for Argonaute 2 in EGFR-KRAS Signaling in Pancreatic Cancer Development. bioRxiv 2017 doi 10.1101/227264.
26. Villaruz LC, Jones H, Dacic S, Abberbock S, Kurland BF, Stabile LP, et al. ATM protein is deficient in over 40% of lung adenocarcinomas. Oncotarget 2016;7(36):57714–25 doi 10.18632/oncotarget.9757. [PubMed: 27259260]
27. Lazarus J, Maj T, Smith JJ, Perusina Lanfranca M, Rao A, D'Angelica MI, et al. Spatial and phenotypic immune profiling of metastatic colon cancer. JCI Insight 2018;3(22) doi 10.1172/jci.insight.121932.

28. Chen S, Wang G, Makrigiorgos GM, Price BD. Stable siRNA-mediated silencing of ATM alters the transcriptional profile of HeLa cells. Biochemical and biophysical research communications 2004;317(4):1037–44 doi 10.1016/j.bbrc.2004.03.149. [PubMed: 15094373]
29. Bild AH, Yao G, Chang JT, Wang Q, Potti A, Chasse D, et al. Oncogenic pathway signatures in human cancers as a guide to targeted therapies. Nature 2006;439(7074):353–7 doi 10.1038/nature04296. [PubMed: 16273092]
30. Staub E An Interferon Response Gene Expression Signature Is Activated in a Subset of Medulloblastomas. Translational Oncology 2012;5(4):297–IN6. [PubMed: 22937182]
31. Drosos Y, Escobar D, Chiang M-Y, Roys K, Valentine V, Valentine MB, et al. ATM-deficiency increases genomic instability and metastatic potential in a mouse model of pancreatic cancer. Scientific Reports 2017;7(1):11144 doi 10.1038/s41598-017-11661-8. [PubMed: 28894253]
32. Sharma S, tenOever BR, Grandvaux N, Zhou GP, Lin R, Hiscott J. Triggering the interferon antiviral response through an IKK-related pathway. Science (New York, NY) 2003;300(5622):1148–51 doi 10.1126/science.1081315.
33. Russell R, Perkhofer L, Liebau S, Lin Q, Lechel A, Feld FM, et al. Loss of ATM accelerates pancreatic cancer formation and epithelial-mesenchymal transition. Nature communications 2015;6:7677 doi 10.1038/ncomms8677.
34. Network CGAR. Integrated Genomic Characterization of Pancreatic Ductal Adenocarcinoma. Cancer cell 2017;32(2):185–203.e13 doi 10.1016/j.ccell.2017.07.007. [PubMed: 28810144]
35. Dewan MZ, Galloway AE, Kawashima N, Dewyngaert JK, Babb JS, Formenti SC, et al. Fractionated but not single-dose radiotherapy induces an immune-mediated abscopal effect when combined with anti-CTLA-4 antibody. Clinical cancer research: an official journal of the American Association for Cancer Research 2009;15(17):5379–88 doi 10.1158/1078-0432.Ccr-09-0265. [PubMed: 19706802]
36. Li X, Yang M, Yu Z, Tang S, Wang L, Cao X, et al. The tyrosine kinase Src promotes phosphorylation of the kinase TBK1 to facilitate type I interferon production after viral infection. Science Signaling 2017;10(460).
37. Hickson I, Zhao Y, Richardson CJ, Green SJ, Martin NMB, Orr AI, et al. Identification and Characterization of a Novel and Specific Inhibitor of the Ataxia-Telangiectasia Mutated Kinase ATM. Cancer Research 2004;64(24):9152–9 doi 10.1158/0008-5472.Can-04-2727. [PubMed: 15604286]
38. Garcia-Diaz A, Shin DS, Moreno BH, Saco J, Escuin-Ordinas H, Rodriguez GA, et al. Interferon receptor signaling pathways regulating PD-L1 and PD-L2 expression. Cell reports 2017;19(6):1189–201. [PubMed: 28494868]
39. Sato H, Niimi A, Yasuhara T, Permata TBM, Hagiwara Y, Isono M, et al. DNA double-strand break repair pathway regulates PD-L1 expression in cancer cells. Nature communications 2017;8(1):1751 doi 10.1038/s41467-017-01883-9.
40. Jiao S, Xia W, Yamaguchi H, Wei Y, Chen MK, Hsu JM, et al. PARP Inhibitor Upregulates PD-L1 Expression and Enhances Cancer-Associated Immunosuppression. Clinical cancer research: an official journal of the American Association for Cancer Research 2017;23(14):3711–20 doi 10.1158/1078-0432.CCR-16-3215.
41. Shen J, Zhao W, Ju Z, Wang L, Peng Y, Labrie M, et al. PARPi triggers the STING-dependent immune response and enhances the therapeutic efficacy of immune checkpoint blockade independent of BRCAness. Cancer Res 2018 doi 10.1158/0008-5472.CAN-18-1003.
42. Vendetti FP, Karukonda P, Clump DA, Teo T, Lalonde R, Nugent K, et al. ATR kinase inhibitor AZD6738 potentiates CD8+ T cell-dependent antitumor activity following radiation. The Journal of clinical investigation 2018;128(9):3926–40 doi 10.1172/jci96519. [PubMed: 29952768]
43. Huang AC, Postow MA, Orlowski RJ, Mick R, Bengsch B, Manne S, et al. T-cell invigoration to tumour burden ratio associated with anti-PD-1 response. Nature 2017;545(7652):60–5 doi 10.1038/nature22079. [PubMed: 28397821]
44. Wartenberg M, Cibin S, Zlobec I, Vassella E, Eppenberger-Castori SMM, Terracciano L, et al. Integrated genomic and immunophenotypic classification of pancreatic cancer reveals three distinct subtypes with prognostic/predictive significance. Clinical cancer research: an official

journal of the American Association for Cancer Research 2018 doi 10.1158/1078-0432.CCR-17-3401.

45. Minn AJ, Wherry EJ. Combination cancer therapies with immune checkpoint blockade: convergence on interferon signaling. Cell 2016;165(2):272–5. [PubMed: 27058661]
46. Kaplan DH, Shankaran V, Dighe AS, Stockert E, Aguet M, Old LJ, et al. Demonstration of an interferon γ-dependent tumor surveillance system in immunocompetent mice. Proceedings of the National Academy of Sciences 1998;95(13):7556–61 doi 10.1073/pnas.95.13.7556.
47. Peng D, Kryczek I, Nagarsheth N, Zhao L, Wei S, Wang W, et al. Epigenetic silencing of TH1-type chemokines shapes tumour immunity and immunotherapy. Nature 2015;527(7577):249–53 doi 10.1038/nature15520. [PubMed: 26503055]
48. Benci JL, Xu B, Qiu Y, Wu TJ, Dada H, Twyman-Saint Victor C, et al. Tumor Interferon Signaling Regulates a Multigenic Resistance Program to Immune Checkpoint Blockade. Cell 2016;167(6): 1540–54.e12 doi 10.1016/j.cell.2016.11.022. [PubMed: 27912061]
49. Sistigu A, Yamazaki T, Vacchelli E, Chaba K, Enot DP, Adam J, et al. Cancer cell-autonomous contribution of type I interferon signaling to the efficacy of chemotherapy. Nat Med 2014;20(11): 1301–9 doi 10.1038/nm.3708. [PubMed: 25344738]
50. Zou W Immunosuppressive networks in the tumour environment and their therapeutic relevance. Nat Rev Cancer 2005;5(4):263–74 doi 10.1038/nrc1586. [PubMed: 15776005]
51. Zou W, Wolchok JD, Chen L. PD-L1 (B7-H1) and PD-1 Pathway Blockade for Cancer Therapy: Mechanisms, Response Biomarkers and Combinations. Science translational medicine 2016;8(328):328rv4–rv4 doi 10.1126/scitranslmed.aad7118.

Significance

This study demonstrates that ATM inhibition induces a type I interferon-mediated innate immune response in pancreatic cancer that is further enhanced by radiation and leads to increased sensitivity to anti-PD-L1 therapy.

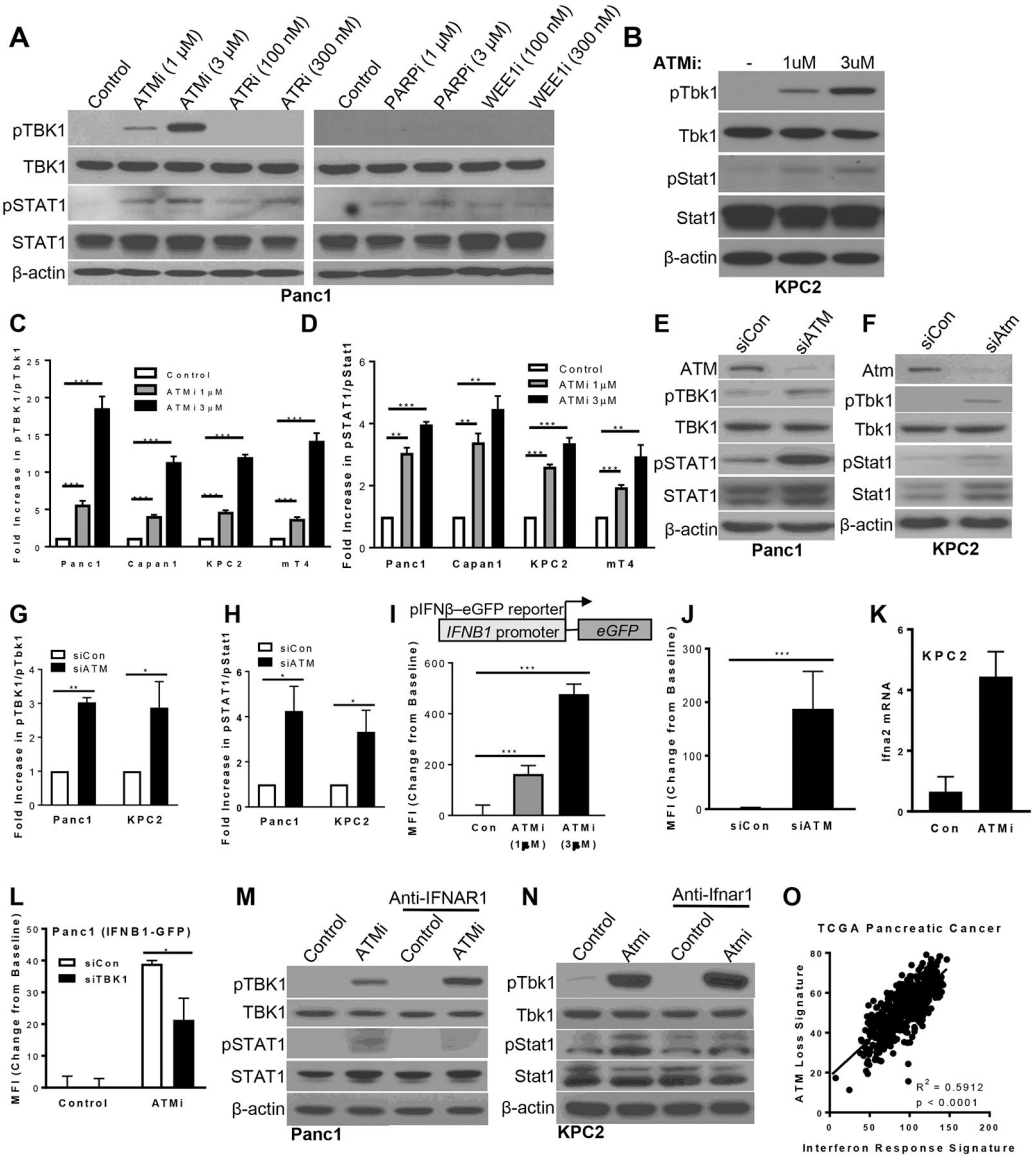

Figure 1: ATM regulates type I interferon signaling in pancreatic cancer.

A, Human Panc1 cells were analyzed by western blot for the indicated proteins at 6 days after the indicated concentrations of ATM inhibitor (KU60019), ATR inhibitor (AZD6738), PARP inhibitor (olaparib), or Wee1 inhibitor (AZD1775). **B**, KPC2 murine pancreatic cells were analyzed by western blot at 6 days after the indicated concentrations of ATM inhibitor (KU60019). **C, D**, Western blots (n = 3) were quantitated for phospho-to-total TBK1 (C) or phospho-to-total STAT1 (D) in the indicated cell lines treated with ATM inhibitor. **E-H**, Panc1 (E) or KPC2 (F) cells were analyzed by western blot 5 days following administration of short interference RNA targeting a scrambled sequence or ATM with quantification illustrated (G, H). **I, J**, Panc1 cells stably transduced with the *IFNB1* promoter reporter (top) were analyzed for GFP mean fluorescent intensity (MFI) following 3 days of treatment with ATM inhibitor (I) or 5 days after siRNA (J). **K**, *Ifn2a* mRNA expression in KPC2 cells was quantitated by PCR analysis following 3 days of treatment with ATM inhibitor. **L**, Panc1-

IFNB1 promotor reporter cells were treated with control or TBK1 siRNA and ATM inhibitor for 5 or 3 days post-treatment, respectively, cells were analyzed for MFI by flow cytometry. **M, N**, Panc1 (M) or KPC2 (N) cells were analyzed by western blot at 3 days of treatment with ATM inhibitor (1uM) with or without human (M) or murine (N) T1IFN receptor blocking antibodies. Statistical significance is indicated P<0.05*, 0.01**, or 0.001*** (C, D, G, H, J). **O**, Correlation between *ATM* loss gene signature and Type I interferon signature in pancreatic TCGA dataset. Pearson correlation coefficients and P values are given.

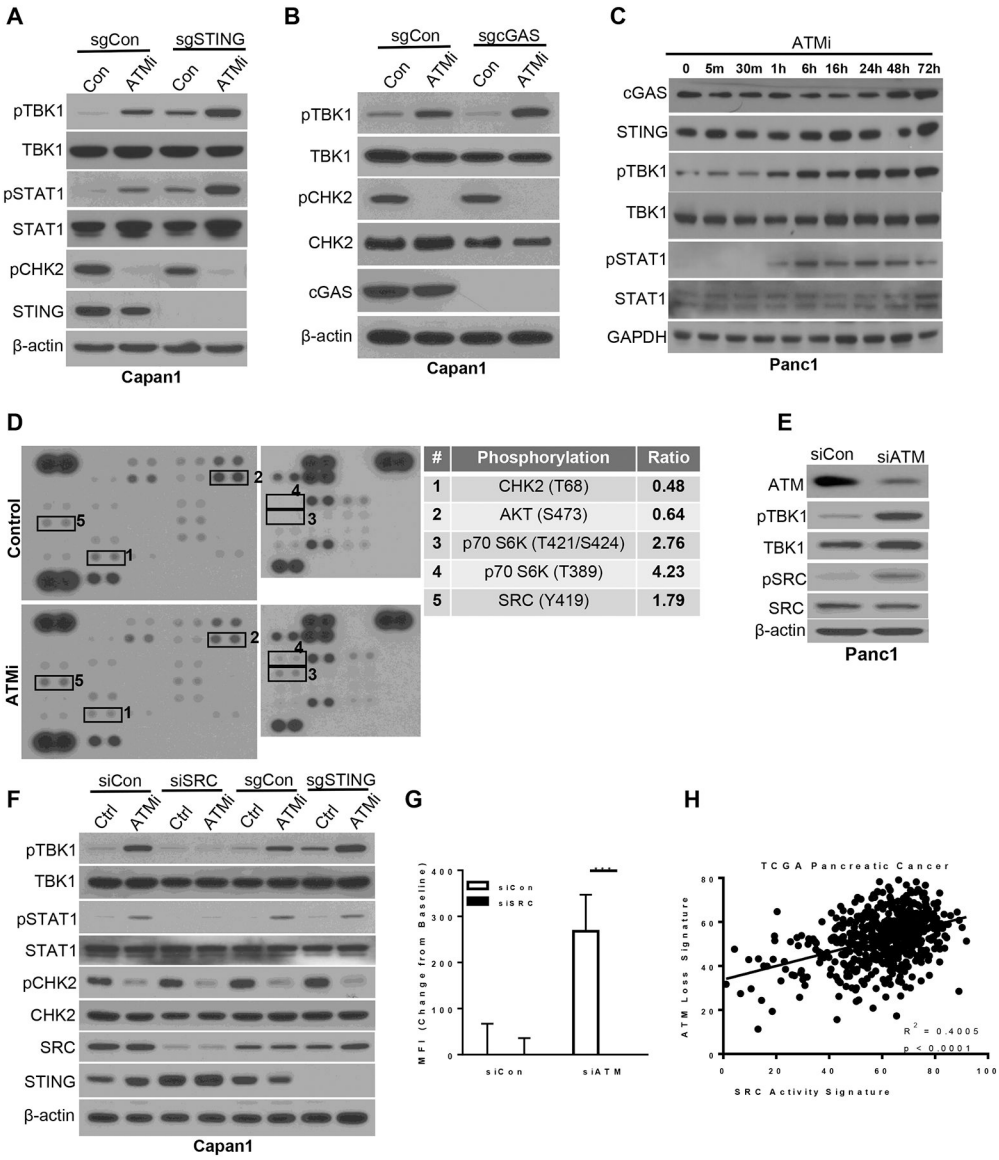

Figure 2: ATM regulation of the type I interferon pathway is STING independent but SRC dependent.

A, STING wild-type (WT) or STING deleted (STING −/−) Capan1 cells generated by CRISPR/Cas9 were analyzed by western blot after 3 days of treatment with ATM inhibitor (1 uM). **B**, cGAS wild-type or cGAS deleted (cGAS −/−) Capan1 cells generated by CRISPR/Cas9 were analyzed by western blot after 3 days of treatment with ATM inhibitor (1 uM). **C**, Panc1 cells were analyzed at indicated times following treatment with ATM inhibitor (1 μM). **D**, Phospho-protein arrays were conducted in Panc1 cells 3 hours after treatment with DMSO or ATM inhibitor (1 μM) with the 5 phospho-proteins demonstrating the greatest change in response to ATM inhibitor indicated. **E**, Panc1 cells were analyzed by western blot 3 days following treatment with control, ATM siRNA and with or without ATM inhibitor (1 μM, F). **F**, Capan1 cells were analyzed by western blot 3 days following treatment with control, SRC siRNA and with or without ATM inhibitor (1 μM). In parallel, WT and STING −/− cells were analyzed by western blot after 3 days of treatment with ATM

inhibitor (1 uM). **G**, Panc1-*IFNB1* promoter reporter cells were analyzed for GFP MFI at 5 days following control, ATM, and/or SRC siRNA. Statistical significance is indicated P<0.05*, 0.01**, or 0.001*** (C, G). **H**, Correlation between *ATM* loss gene signature and *SRC* gene signature in pancreatic TCGA dataset. Pearson correlation coefficients and P values are given.

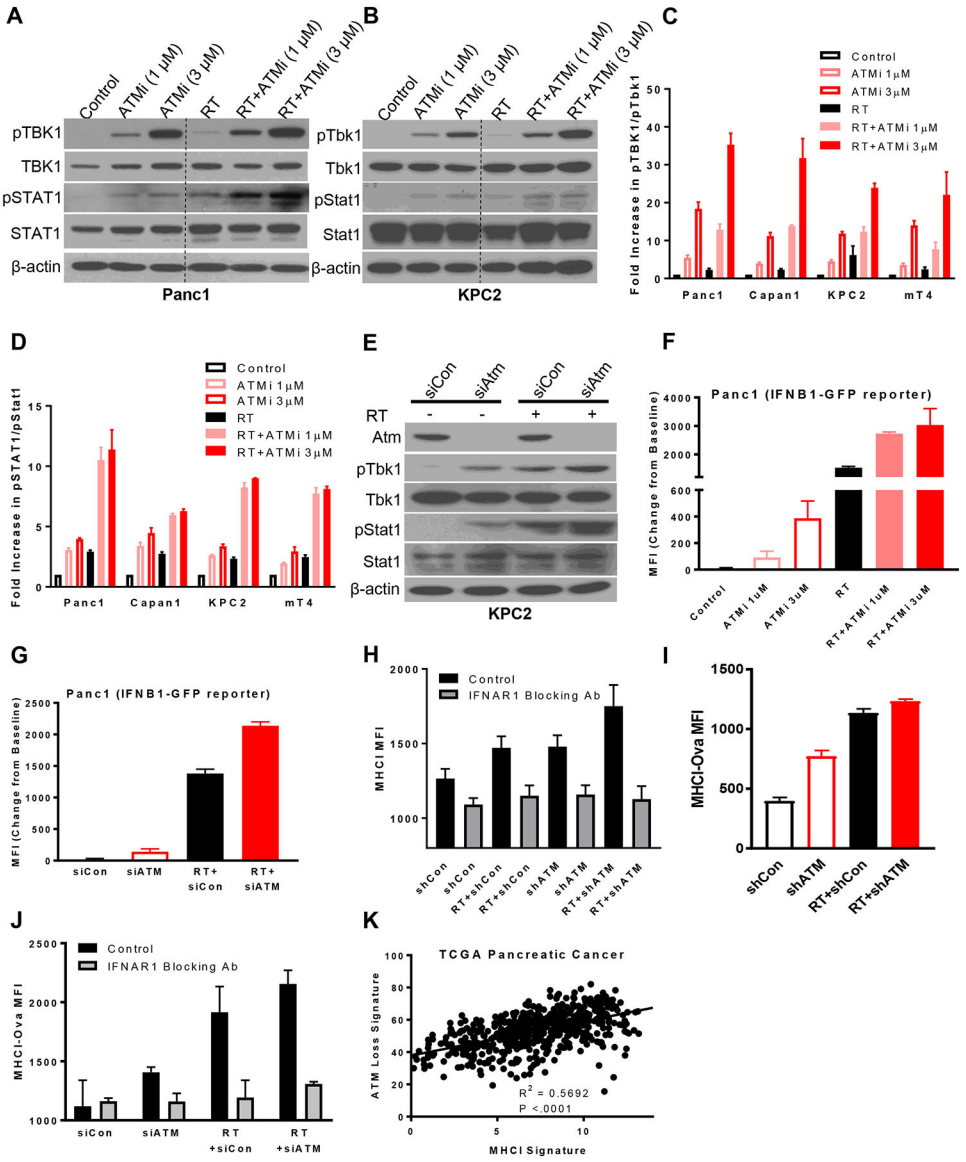

Figure 3: ATM inhibition cooperates with radiation to activate type I interferon signaling.

A, B, Panc1 (A) or KPC2 (B) cells were analyzed by western blot at 6 days following radiation (20 Gy) and treatment with the indicated concentrations of ATM inhibitor. **C, D**, Western blots (n = 3) were quantitated for phospho-to-total TBK1 (C) or phospho-to-total STAT1 (D) in the indicated cell lines treated with radiation (20 Gy) and/or ATM inhibitor. **E**, KPC2 cells were analyzed by western blot at 3 days following treatment with control of ATM siRNA and 2 days post-radiation (20 Gy). **F, G**, Panc1-*IFNB1* promotor reporter cells were analyzed for GFP MFI following at 3 days after radiation (8 Gy) and/or treatment with ATM inhibitor (F) or at 5 days post-treatment with siRNA (G). **H**, Bone marrow derived macrophages were co-cultured with the supernatant of control or Atm shRNA mT4 cells that were treated with radiation (8 Gy) and/or T1IFN receptor blocking antibodies. MHCI was measured as MFI by flow cytometry. **I, J**, mT4 cells stably expressing ovalbumin and control or ATM shRNA were treated with RT (8 Gy) and in some conditions IFNAR1

blocking antibody (J) and analyzed by flow cytometry for MHCI-Ova (SINFEKKL) complexes. **K**, Correlation between *ATM* loss gene signature and *SRC* gene signature in pancreatic TCGA dataset. Pearson correlation coefficients and P values are given.

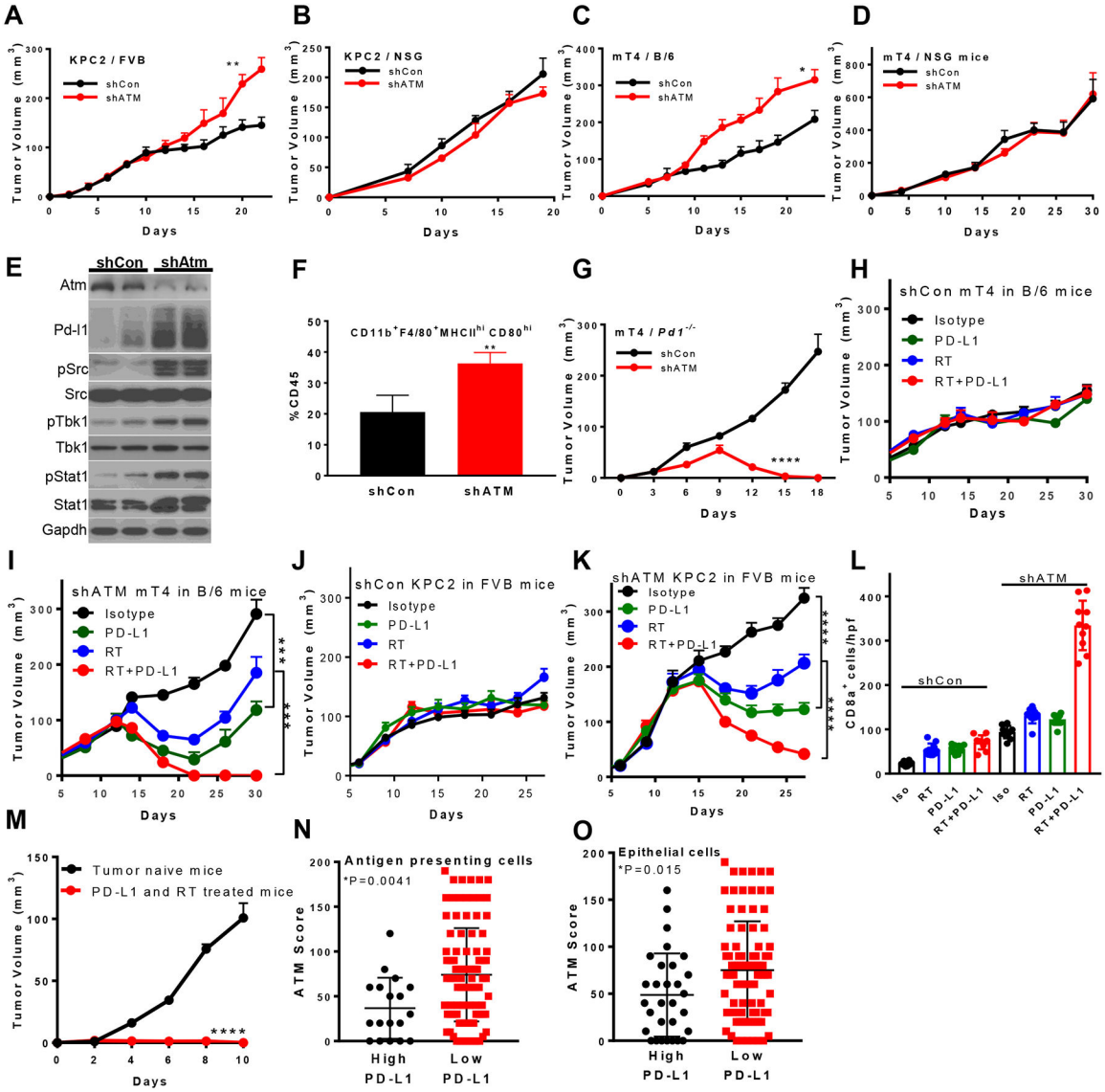

Figure 4: ATM regulates pancreatic tumor immunity and ICB efficacy in vivo.

A, C, KPC2 (A) or mT4 (C) tumors were inoculated in FVB/NJ (A) or C57Bl/6 mice (C) and tumor growth was monitored (shCon n = 5; shATM, n = 5). **B, D**, ATM wild type or silenced KPC2 (B) or mT4 (D) tumors were inoculated in NSG mice and tumor growth was monitored shCon, n = 5; shATM, n = 5. **E**, KPC2 tumors of the indicated genotypes were analyzed by western blot at 10 days post-implantation. **F**, Tumor associated macrophages from established KPC2 tumors were analyzed by flow cytometry. **G**, The effect of host Pd1$^{-/-}$ status on subcutaneous tumor growth was assessed by implanting mT4 tumors in C57/Bl6 Pd1$^{-/-}$ mice (shCon, n = 10; shATM, n = 10). **H-K**, shCon (H, J) or shATM (I, K) mT4 (H, I) or KPC2 (J, K) tumors were implanted in C57/Bl6 or FVB mice, respectively, that were subsequently treated with anti-PD-L1 (100ug, QD3), radiation (8 Gy), or the combination (n = 10–12 per treatment arm). **L**, CD8a+ cells / hpf in KPC2 tumors were quantified following treatment as described in H with each arm representing a minimum of 10 fields from at least 3 tumors. **M**, Naïve mice (n = 8) and mice treated with RT+anti-PD-

L1 (n = 5) as in panel G were re-inoculated with mT4 cells. **N, O**, PD-L1 expression on antigen presenting cells (N) and epithelial cells (O) in a human pancreatic tumor TMA was analyzed as a function of ATM expression. Statistical significance is indicated P<0.05*, 0.01**, or 0.001***, 0.0001****.